Ordered Arrays Generated via Metal-Initiated Self-Assembly of Terpyridine Containing Dendrimers and Bridging Ligands

Diego J. Díaz, Gregory D. Storrier, Stefan Bernhard, Kazutake Takada, and Héctor D. Abruña*

Department of Chemistry and Chemical Biology, Baker Laboratory, Cornell University, Ithaca, New York, 14853-1301

Received April 27, 1999

The interfacial reaction of the terpyridyl-pendant dendrimers (dend-*n*-tpy; $n = 4, 8, 32$) and of the bridging ligand 1,4-bis[4,4″-bis(1,1-dimethylethyl)-2,2′:6′,2″terpyridine-4′-yl]benzene (BBDTB) dissolved in CH_2Cl_2 with aqueous Fe^{2+} or Co^{2+} gives rise to film formation on highly oriented pyrolytic graphite surfaces. Molecularly resolved scanning tunneling microscopy (STM) images reveal that these films form highly ordered 2-D hexagonal arrays which appear to be composed of one-dimensional polymeric strands with a repeat unit of $(\text{tpy-dend-tpy-M})_x$ in the case of dendrimers or $(\text{tpy-bridge-tpy-M})_x$ in the case of BBDTB ($M = Fe^{2+}$, Co^{2+}). The extension of the ordered domains appears to be delimited by terrace width. The dimensions obtained from an analysis of STM images is consistent with the size of the dendrimer or the bridging ligand (obtained from molecular modeling) from which the films are derived. In the case of films derived from dend-*n*-tpy the ordering is dependent on the dendrimer generation. In all cases, the films are electrochemically active and exhibit a reversible wave at a formal potential that corresponds to the respective $[M(tpy)_2]^{2+}$ complex.

Dendrimers have received much attention in recent times since they form in well-defined patterns that allow control over molecular weight, topology, cavity size, and surface functionality.[1−5] Because of this ability to deliberately control size and functionality, dendrimers have been incorporated into applications such as molecular recognition,[5,6] sensing devices,[7,8] and photosensitive materials.[9−11] Films of dendrimers on surfaces have been prepared by a variety of methods including self-assembly, surface confinement, and spin coating.[12] The modification of electrode surfaces with redox-active dendrimers could provide valuable insights not only for understanding interfacial redox reactions but also in applications where they could be employed as electron-transfer mediators, catalysts, sensors, electrochromic and electronic devices. Moreover, the possibility of controlling the surface structure of layers of dendrimers on electrode surfaces could open up novel opportunities in nanotechnology. Recent studies on dendrimers containing redox-active centers based on transition metal complexes as well as organometallic species[13,14] point to their potential use as electrode surface modifiers. There is also a continuing interest in the use of bridging ligands for the preparation of materials of deliberately designed electrical, electrochemical, and spectroscopic properties.[15]

The deliberate control over surface structure requires a detailed understanding of dendrimer/dendrimer and dendrimer/substrate interactions as well as knowledge of the dendrimer structure in the solid state. Most experimental approaches have not been able to provide direct visualization of the structure of adsorbed layers of dendrimers on surfaces at the molecular level. Because of the lack of X-ray crystallographic data on these types of materials, investigators have relied on theoretical models to provide insight on their structure, their conformation in solution, and their self-assembly on surfaces and at interfaces.[12,16] The ability to obtain molecularly resolved images of dendrimers on surfaces could provide a great deal of insight into how these processes occur at the microscopic level and on the nature of the interactions.

(1) Newkome, G. R.; Moorefield, C. N.; Vögtle, F. *Dendritic Molecules: Concepts, Syntheses, Perspectives*; VCH: Weinheim, 1996.
(2) Matthews, O. A.; Shipway, A. N.; Stoddart, J. F. *Prog. Polym. Sci.* **1998**, *23*, 1−56.
(3) Fréchet, J.-M. J. *Science* **1994**, *263*, 1710−1715.
(4) Tomalia, D. A.; Naylor, A. M.; Goddard, W. A., III *Angew. Chem., Int. Ed. Engl.* **1990**, *29*, 138−175.
(5) Zeng, F.; Zimmerman, S. C. *Chem. Rev.* **1997**, *97*, 1681−1712.
(6) Newkome, G. R.; Woosley, B. D.; He, E.; Moorefield, C. N.; Güther, R.; Baker, G. R.; Escamilla, G. H.; Merrill, J. *J. Chem. Soc., Chem. Commun.* **1996**, 2737−2738.
(7) Zhao, M.; Tokuhisa, H.; Crooks, R. M. *Angew. Chem., Int. Ed. Engl.* **1997**, *36*, 2596−2600.
(8) Valério, C.; Fillaut, J. L.; Ruiz, J.; Guittard, J.; Blais, J. C.; Astruc, D. *J. Am. Chem. Soc.* **1997**, *119*, 2588−2589.
(9) Balzani, V.; Campagna, S.; Genti, G.; Juris, A.; Serroni, S.; Venturi, M. *Acc. Chem. Res.* **1998**, *31*, 759−833.
(10) Bar-Haim, A.; Klafter, J. *J. Phys. Chem. B* **1998**, *102*, 1662−1664.
(11) (a) Jiang, D. L.; Aida, T. *Nature* **1997**, 388, 454−456. (b) Junge, D. M.; McGrath, D. V. *J. Chem. Soc., Chem. Commun.* **1997**, 857−858.
(12) Tsukruk, V. V. *Adv. Mater.* **1998**, *10*, 253−257 and references therein.
(13) (a) Takada, K.; Díaz, D. J.; Abruña, H. D.; Cuadrado, I.; Casado, C.; Alonso, B.; Morán, M.; Losada, J. *J. Am. Chem. Soc.* **1997**, *119*, 10763−10773. (b) Alonso, B.; Morán, M.; Casado, C. M.; Lobete, F.; Losada, J.; Cuadrado, I. *Chem. Mater.* **1995**, *7*, 1440−1442.
(14) (a) Van Veggel, F. C. J. M.; Huck, W. T. S.; Reinhoudt, D. N. *Macromol. Symp.* **1998**, *131*, 165−173. (b) Gorman, C. *Adv. Mater.* **1998**, *10*, 4, 295. (c) Frey, H.; Lach, C.; Lorenz, K. *Adv. Mater.* **1998**, *10*, 4, 279−294. (d) Bryce, M. R.; Devonport, W. *Adv. Dendritic Macromol.* **1996**, *3*, 115−149.
(15) (a) Grosshenny, V.; Harriman, A.; Ziessel, R. *Angew. Chem., Int. Ed. Engl.* **1995**, *34*, 1100. (b) Balzani, V.; Barigelletti, F.; Belser, P.; Bernhard, S.; De Cola, L.; Flamigni, L. *J. Phys. Chem.* **1996**, *100*, 16786−8. (c) De Cola, L.; Balzani, V.; Barigelletti, F.; Flamigni, L.; Belser, P.; Bernhard, S. *Recl. Trav. Chim. Pays-Bas* **1995**, *114*, 534−41. (d) Belser, P.; von Zelewsky, A.; Frank, M.; Seel, C.; Vögtle, F.; De Cola, L.; Barigelletti, F.; Balzani, V. *J. Am. Chem. Soc.* **1993**, *115*, 4076. (e) Barigelletti, F.; Flamigni, L.; Balzani, V.; Collin, J.-P.; Sauvage, J.-P.; Sour, A.; Constable, E. C.; Cargill Thompson, A. M. W. *J. Am. Chem. Soc.* **1994**, *116*, 7692.
(16) (a) Mansfield, M. L. *Polymer* **1996**, *37*, 3835−3841. (b) Hudson, S. D.; Jung, H. T.; Percec, V.; Cho, W. D.; Johansson, G.; Ungar, G. *Science* **1997**, *278*, 449−451.

10.1021/la990513n CCC: $18.00 © 1999 American Chemical Society
Published on Web 08/05/1999

We recently carried out a comprehensive study of ferrocenyl-containing dendrimers[13] utilizing cyclic voltammetry and the electrochemical quartz crystal microbalance (EQCM). These dendrimers were found to adsorb onto platinum surfaces, and we characterized the thermodynamics and kinetics of adsorption. Furthermore, we were able to obtain molecularly resolved images of the dendrimer containin 64 ferrocenyl units adsorbed onto a Pt(111) surface using tapping-mode atomic force microscopy (TMAFM).

Most recently[17a] we have synthesized and characterized pyridine (py), 2,2′-bipyridine (bpy), and 2,2′:6′,2″-terpyridine (tpy) containing dendrimers with 4, 8, 16, 32, and 64 coordinating groups on their periphery. Complexation of the chelating groups with appropriate ruthenium(II) precursor complexes yielded dendrimers surface functionalized with tris(bipyridyl) ruthenium(II) or bis(terpyridyl) ruthenium(II) pendant complexes. The redox behavior, adsorption thermodynamics and kinetics have been studied by electrochemical and EQCM techniques.[17b]

Here we show that the interfacial reaction of the terpyridine-pendant dendrimers (dend-*n*-tpy, $n = 4$, 8, 32) and of the bridging ligand 1,4-bis[4,4″-bis(1,1-dimethylethyl)-2,2′:6′,2″-terpyridine-4′-yl]benzene (BBDTB) dissolved in CH_2Cl_2 with aqueous Fe^{2+} or Co^{2+} gives rise to ordered film formation on HOPG (highly oriented pyrolytic graphite) surfaces. We describe film formation and the characterization of the films via scanning tunneling microscopy (STM) and electrochemical methods.

Dend-*n*-tpy (where $n = 4$, 8, 16, 32, 64) compounds were prepared as described previously[17a] through the peptide coupling of a carboxylic acid-pendant terpyridine ligand with the appropriate poly(amido amine) (PAMAM) starburst dendrimer. A representative molecular structure of dend-8-tpy is depicted in Figure 1a. BBDTB was synthesized following published procedures,[18] and its structure is depicted in Figure 1b. The ability of terpyridine ligands to coordinate transition metal ions is well-known.[19] We were interested in the preparation of highly ordered films of these materials and chose to investigate the interfacial (at the CH_2Cl_2/water interface) formation of Fe^{2+} and Co^{2+} complexes of these terpyridine containing materials since the formation of the $[M(tpy)_2]^{2+}$ complexes ($M = Fe^{2+}$, Co^{2+}) is characterized by having large formation constants and facile kinetics.[19]

Films were prepared by bringing into contact a 0.02 mM solution of the dendrimer or BBDTB in CH_2Cl_2 with aqueous $FeSO_4$ or $CoSO_4$ (0.1 M) on the surface of a freshly cleaved HOPG substrate (ZYA Grade, Union Carbide). The reaction was allowed to proceed at room temperature for 18 h. The surface was then thoroughly rinsed with H_2O and CH_2Cl_2 to remove excess reactants.

STM images were obtained in air using a Molecular Imaging 10 μm scanner, Molecular Imaging isolation chamber, and Digital Instruments Nanoscope E Controller. All images shown are unfiltered, taken on-line, and no off-line zoom was used. Bias voltages between +140 and +200 mV and setpoint currents between 1.0 and 2.0 nA were employed. The scan rates were between 4 Hz for the larger scale images and 15 Hz for the smaller size images. The images are taken at 512 samples resolution to obtain better detailed images.

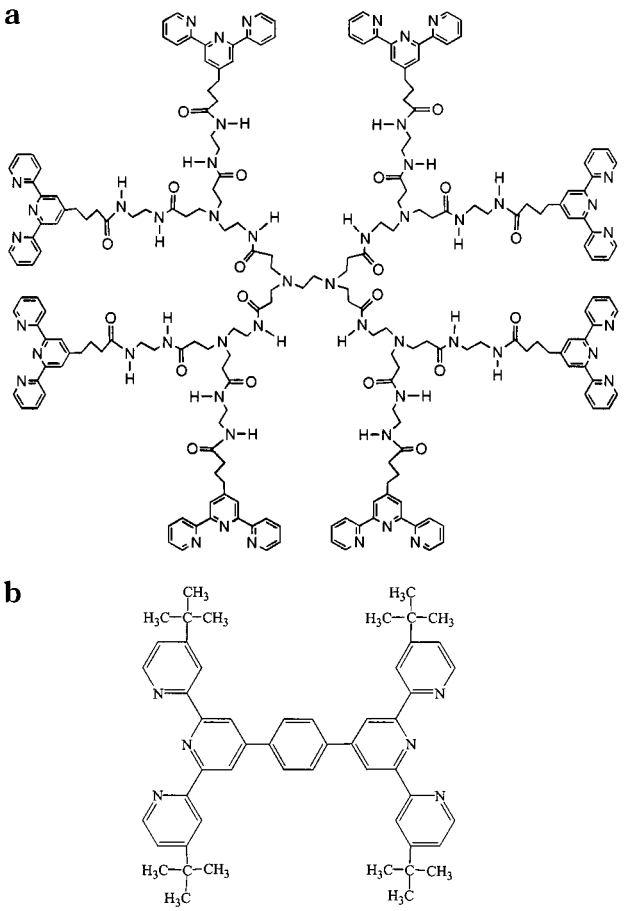

Figure 1. (a) Molecular structure of dend-8-tpy. (b) Molecular structure of BBDTB.

Most of the studies were carried out with the dend-8-tpy/Fe^{2+} system, and thus these results are discussed in detail below and then compared with those obtained with dend-4-tpy, dend-32-tpy, and BBDTB. Figure 2a shows a 550 × 550 nm image of a film derived from the dend-8-tpy/Fe^{2+} combination where it is immediately apparent that well-defined structures form over relatively extensive areas. While some 3-D clusters appear to form, particularly at step edges, there are extensive regions of the HOPG substrate covered by a well-organized film. In contrast, images of the dend-8-tpy in the absence of a metal center (to which the terpyridine units could coordinate) adsorbed on an HOPG substrate (by evaporation of a 0.02 mM CH_2Cl_2 solution) exhibited only large irregular clusters which were easily dragged by the tip so that no stable image could be obtained independent of changes in the imaging conditions. Figure 2b shows a close up of part of the ordered regions apparent in Figure 2a and illustrates the hexagonal packing on the HOPG surface. Similar highly ordered hexagonal arrays could be obtained by viewing virtually any of the ordered regions.

The substrate structure appears to play a role in the formation of well-ordered films. Whereas larger substrate imperfections appear to be covered by 3-D clusters, STM images show that the size of the ordered domains is dependent on terrace width and delimited by step edges on the substrate. This is evident in panels c and d of Figure 2. Figure 2c shows that the highly ordered domain is delimited by the terrace dimensions. A closeup of the step edge (Figure 2d) shows that it is decorated by what appears to be a one-dimensional array of the complex (akin to a string of pearls). This decoration closely follows the step features as shown in the center of Figure 2d and suggests

(17) (a) Storrier, G.; Takada, K.; Abruña, H. D. *Langmuir* **1999**, *15*, 872−884. (b) Takada, K.; Storrier, G.; Morán, M.; Abruña, H. D. *Langmuir*, in press.

(18) (a) Constable, E. C.; Cargill Thompson, A. M. W. J. *J. Chem. Soc., Dalton Trans.* **1992**, 3467−75. (b) Fife, W. K. *J. Org. Chem.* **1983**, *48*, 1375−77.

(19) McWhinnie, W. R.; Miller, J. D. *Adv. Inorg. Chem. Radiochem.* **1969**, *12*, 135−215.

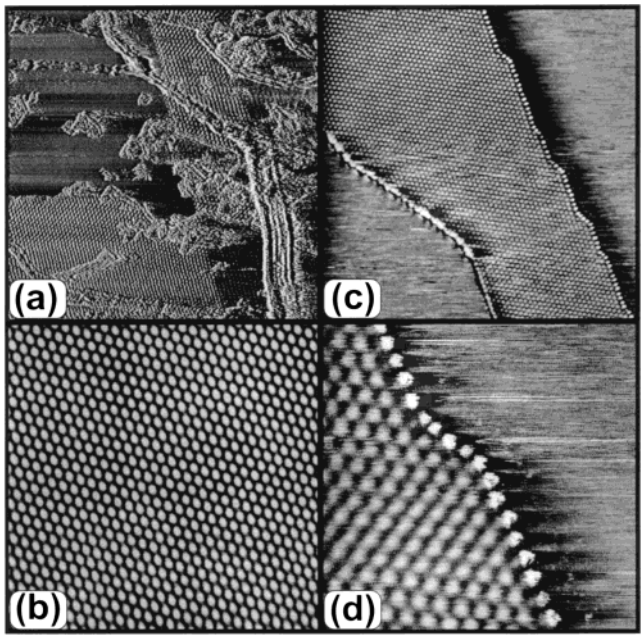

Figure 2. Unfiltered STM images of dend-8-tpy/Fe^{2+} on HOPG. (a) 550 × 550 nm STM image where the assembly of well-ordered arrays and 3-D clusters on the HOPG surface are evident. (b) 200 × 200 nm image featuring a highly ordered 2-D hexagonal domain. (c) 304 × 304 nm image of a well-ordered domain being delimited by the substrate's step edges. (d) 69 × 69 nm image of the dendrimer film along the step edges. Imaging conditions (scanning mode, bias, setpoint current): (a) constant height, 200 mV, 1.70 nA; (b) constant current, 150 mV, 1.70 nA; (c) constant height, 146 mV, 1.5 nA; (d) constant height, 199 mV, 1.5 nA.

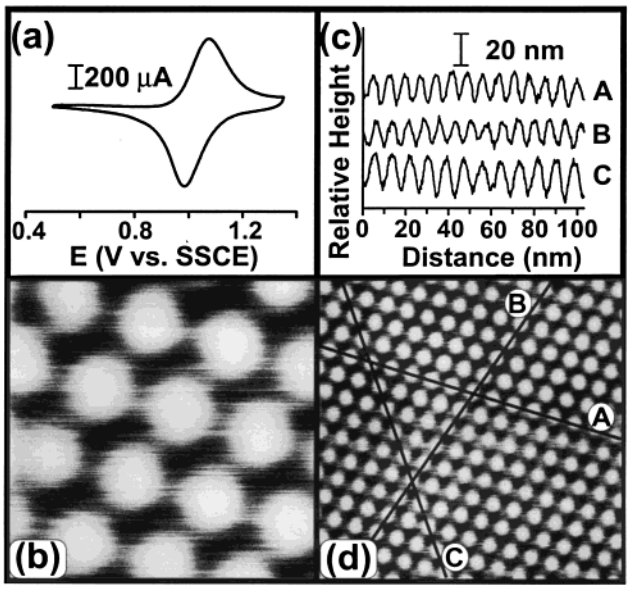

Figure 3. (a) Cyclic voltammogram at 50 mV/s of a dend-8-tpy/Fe^{2+}-modified HOPG electrode in CH_3CN, 0.1 M TBAP. (b) High-resolution STM image (26 × 26 nm, unfiltered) of dend-8-tpy/Fe^{2+} on HOPG. (c) Section analyses of dendrimer film in the alignments depicted in panel d. (d) 105 × 105 nm image illustrating the alignments of the section analyses. Imaging conditions (scanning mode, bias, setpoint current): (b) constant current, 150 mV, 1.70 nA; (d) constant current, 150 mV, 1.70 nA.

that the highly ordered regions within the terraces are likely the result of 2-D packing of 1-D strands where the repeat unit would ostensibly be (**tpy**-dend-$(tpy')_6$-**tpy**-$Fe^{2+})_x$ (where **tpy** = terpyridine that bridges (via coordination to an Fe^{2+} center) two dendrimer molecules and tpy′ = terpyridine not coordinated to an Fe^{2+} center).

The cyclic voltammogram, in acetonitrile/0.1 M TBAP (tetra-*n*-butylammonium perchlorate), of the dendrimer-modified HOPG electrode (Figure 3a) exhibits a well-defined reversible redox couple with an $E^{\circ\prime}$ value of +1.03 V vs SSCE (saturated sodium calomel electrode)—a value that is very close to that reported for $[Fe(tpy)_2]^{2+}$ ($E^{\circ\prime}$ = +1.10 V vs SSCE[20]) and unambiguously establishes the nature of the immobilized complex. Although the total amount of redox-active material immobilized on the surface could be determined from the charge under the voltammetric wave, further analysis is precluded by the fact that the coverage is largely not uniform as can be ascertained from Figure 2a.

The hexagonal packing of a highly ordered region is clearly evident in the high-resolution image shown in Figure 3b. Close inspection and section analysis of such images (panels c and d of Figure 3) show that in these hexagonal arrays the intermolecular distances are equivalent along two directions (A, B) but different (longer) along the third (C). These differences in packing (intermolecular distances) are consistent with the 2-D packing of 1-D strands as suggested above. The packing is thus better described as quasi-hexagonal.

The STM images (which were relatively insensitive to changes in imaging conditions such as bias) of these dendrimer films are very stable and can be repeatedly imaged with virtually no degradation of the image quality. This is in stark contrast to most, if not all, reports of images of dendrimers on surfaces.[21] This reproducibility suggests that there are strong intermolecular interactions and that these could likely be responsible for the stability of these ordered domains. This stability has allowed us to obtain very high resolution images (all the images presented are unfiltered) that we believe are the highest resolution images reported for dendrimer films to date.

The sizes of these dendrimers are also in good agreement with values obtained by simple calculations (using the modeling program HYPERChem) which suggest a size of approximately 5 nm while values obtained from STM images are in the range 5.0−6.0 nm. A more precise determination by scanned probe techniques is difficult since finite size limitations arise due to a convolution of tip and sample geometries. Although the size agreement is reasonably good, some tip-to-sample convolution might still exist.

Images reminiscent of those presented here have been previously reported for HOPG alone and have been ascribed to Moiré patterns arising from a small-angle rotation (misorientation) between the top and underlying layer(s) of the HOPG substrate.[22−24] This rotation creates an angle-dependent superperiodicity P ($P = 2.45$ Å/2 sin(θ/2), where θ is the angle between the hexagonal lattices) that is superimposed on the HOPG image. Most recently, it has been proposed that other factors may also be involved.[25] However, based on the properties of these Moiré

(20) Arana, C.; Yan, S.; Keshavarz K. M.; Potts, K. T.; Abruña, H. D. *Inorg. Chem.* **1992**, *31*, 3680−3682.

(21) Sheiko, S. S.; Eckert, G.; Ignat'eva, G.; Muzafarov, A. M.; Spickerman, J.; Räder, H. J.; Möller, M. *Macromol. Rapid Commun.* **1996**, *17*, 283−297.

(22) Kuwabara, M.; Clarke, D. R.; Smith, D. A. *Appl. Phys. Lett.* **1990,** *56*, 2396−2398.

(23) Liu, C.; Chang, H.; Bard, A. J. *Langmuir* **1991**, *7*, 1138−1142.

(24) Xhie, J.; Sattler, K.; Ge, M. Venkateswaran, N. *Phys. Rev. B* **1993**, *47*, 15835−15841.

(25) Cee, V. J.; Patrick, D. L.; Beebe, T. P. *Surf. Sci.* **1995**, *329*, 141−148.

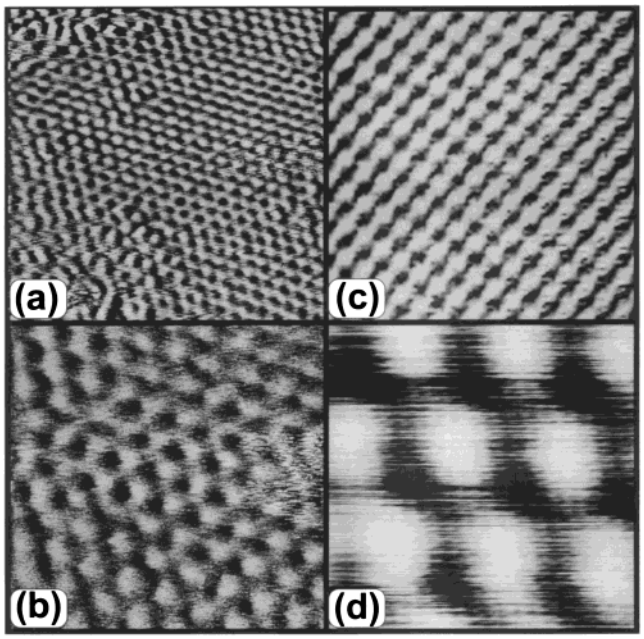

Figure 4. (a) Medium-resolution STM image (52 × 52 nm, unfiltered) of dend-4-tpy/Fe^{2+} on HOPG. (b) High-resolution STM image (23 × 23 nm) of the film presented in panel a. (c) Medium-resolution STM image (40 × 40 nm, unfiltered) of films derived from BBDTB/Fe^{2+} on HOPG. (d) High-resolution STM image (9.3 × 9.3 nm) of the film presented in panel c. Imaging conditions (scanning mode, bias, setpoint current): (a) constant current, 216 mV, 1.03 nA; (b) constant current, 216 mV, 1.03 nA; (c) constant current, 500 mV, 1.46 nA; (d) constant current, 500 mV, 1.00 nA,

images, particularly their bias dependency and their variable periodicity, we can unambiguously rule them out as being responsible for the images reported here (see Supporting Information).

As mentioned above, we believe that these films are composed of hexagonally packed 1-D chains. The question then arises as to why should such structures form at all given that the formation of $[Fe(tpy)_2]^{2+}$ is kinetically facile, the formation constant has a large value, and there are eight terpyridine units per dendrimer molecule. We believe that a combination of factors might be responsible for this. First of all it should be recalled that the reaction is taking place at the interface between two immiscible liquids, and although the interface has a finite thickness, the reaction in two dimensions is favored. However, it is also clear that 3-D clusters also form as is evident in Figure 2a. The formation of layers, where each dendrimer is bound to four neighbors in an approximately rectangular array, would appear to be kinetically and/or sterically hindered. On the other hand, the packing of 1-D chains would appear to be less inhibited. Thus, although the formation of two- and three-dimensional structures likely takes place, the formation of highly ordered films of packed 1-D chains would appear to be favored.

It should also be mentioned that in some cases we have been able to observe films (although their occurrence was much less prevalent) where the dendrimers appear to be bound to four neighbors giving rise to STM images with the dendrimer units in a rectangular array.

Highly ordered films have also been obtained for dend-4-tpy/Fe^{2+}. Panels a and b of Figure 4 show STM images (52 × 52 and 23 × 23 nm, respectively) of a film prepared in a way analogous to that described above for dend-8-tpy/ Fe^{2+}. In this case although the images are not as sharply defined, they are qualitatively very similar. In addition the size of the dendrimer units is approximately 2.7 nm in diameter, which is consistent with the smaller size of dend-4-tpy relative to dend-8-tpy and is also consistent with results from computer modeling.

Studies with larger dendrimers such as dend-32-tpy, containing 32 terpyridines on the periphery of the molecule, show that they have a higher tendency to form 3-D structures, attributed to the larger number of terpyridyl groups oriented toward the interface. Other factors, such as the metal ion concentration and the structure of the substrate, appear to be important in controlling the structure of these films. Such effects are currently under study.

It should also be mentioned that although the use of Fe^{2+} complexes was emphasized in this study, we have also prepared very similar films using Co^{2+} which, similar to Fe^{2+}, has facile kinetics of complex formation and a large formation constant.

Given that in the formation of the ordered arrays only two of the terpyridine ligands are ostensibly bound to a metal center, it should be possible to prepare ordered structures with ligands that have two terpyridine units separated by a bridge. With that purpose in mind we synthesized the bis-terpyridine bridging ligand BBDTB presented in Figure 1b. Following the same procedure used in the preparation of films based on the terpyridine-containing dendrimers, we have been able to prepared highly ordered arrays of the Fe^{2+} complex. STM images of such a film are presented in panels c and d of Figure 4. Again, highly ordered arrays are obtained, and the dimensions are consistent with the size of the ligand. This points to the degree of control that can be achieved by suitable modification of the ligand.

The STM studies described here have provided useful insights on the formation of highly ordered structures derived. For example they suggest that in the case of the dend-*n*-tpy/M^{2+} that although a truly 2-D array is likely to be more thermodynamically stable, the 1-D chains appear to be the kinetically controlled product/structure. The interfacial approach employed appears very promising for the formation of structures of deliberate architecture. For example it might be possible to generate 2-D as well as 3-D arrays. Moreover one could generate heterometallic structures in such cases. Those studies are being currently pursued.

Acknowledgment. This work was supported by the Office of Naval Research and the Cornell Center for Materials Research (CCMR). D.J.D. acknowledges support by a Graduate School Fellowship from Cornell University, the CCMR, and the Ford Foundation. S.B. acknowledges support by the Swiss National Science Foundation.

Supporting Information Available: STM images of the dendrimer films on HOPG and comparison with images obtained from freshly cleaved HOPG where superperiodicities ascribed to Moiré patterns are apparent. This material is available free of charge via the Internet at http://pubs.acs.org.

LA990513N